Antarctic Science 22(6), 603–618 (2010) doi:10.1017/S0954102010000799

Cosmogenic nuclide exposure age constraints on the glacial history of the Lake Wellman area, Darwin Mountains, Antarctica

B.C. STOREY[1], D. FINK[2], D. HOOD[1], K. JOY[1], J. SHULMEISTER[3], M. RIGER-KUSK[1] and M.I. STEVENS[4]

[1]*Gateway Antarctica, University of Canterbury, Private Bag 4800, Christchurch, New Zealand*
[2]*Institute for Environmental Research, ANSTO, PMB1, Menai 2234, Australia*
[3]*Geography, Planning and Environmental Management, University of Queensland, St Lucia 4072, Australia*
[4]*South Australian Museum, SA 5000, and School of Earth and Environmental Sciences, University of Adelaide, SA 5000, Adelaide, Australia*
Bryan.storey@canterbury.ac.nz

Abstract: We present direct terrestrial evidence of ice volume change of the Darwin and Hatherton glaciers which channel ice from the Transantarctic Mountains into the Ross Ice Shelf. Combining glacial geomorphology with cosmogenic exposure ages from 25 erratics indicates a pre-LGM ice volume at least 600 m thicker than current Hatherton ice elevation was established at least 2.2 million years ago. In particular, five erratics spread across a drift deposit at intermediate elevations located below a prominent moraine feature mapped previously as demarcating the LGM ice advance limits, give a well-constrained single population with mean ^{10}Be age of 37.0 ± 5.5 ka (1σ). At lower elevations of 50–100 m above the surface of Lake Wellman, a further five samples from within a younger drift deposit range in exposure age from 1 to 19 ka. Our preferred age model interpretation, which is partly dependent on the selection of a minimum or maximum age-elevation model, suggests that LGM ice volume was not as large as previously estimated and constrains LGM ice elevation to be within ± 50 m of the modern Hatherton Glacier ice surface, effectively little different from what is observed today.

Received 9 March 2010, accepted 30 August 2010

Key words: cosmogenic exposure dating, Last Glacial Maximum, Latitudinal Gradient Project

Introduction

The spatial and temporal evolution of past Antarctic ice sheets has had a major influence on the development of polar ecosystems within ice-free regions of Antarctica. The cycle of advance and retreat of Antarctic ice sheets would have necessarily eradicated most terrestrial life during ice sheet maxima with recolonization following their retreat and possibly longer-term preservation of only a very small subset of flora and fauna (Adams *et al*. 2006, Stevens *et al*. 2006, Convey & Stevens 2007, Convey *et al*. 2008). On the assumption that major continental ice sheet advances, including the Last Glacial Maximum (LGM), overran ice-free habitats and coastal oases, most terrestrial life would have been wiped out, with the exception of sub-surface bacteria. On this basis, one can then postulate that there may be a relationship between the biodiversity of a glacial landscape and its glacial history. A few ice-free terrestrial environments, such as the McMurdo Dry Valleys region, have existed within the Transantarctic Mountains for up to 10–12 million years (Sugden *et al*. 2006), although many more are likely.

However, in order to investigate the idea of a correlation between ice sheet size and biodiversity, the large uncertainties in the extent and thickness of formerly expanded ice sheets (Bentley 1999), particularly at the LGM (Mackintosh *et al*. 2007) require attention. Computer models of the past behaviour of the Antarctic ice sheet based on glaciological, marine and physical inputs have provided conflicting pictures (Bentley 1999, Denton & Hughes 2002, Huybrechts 2002). Confounding these efforts is the scarcity of terrestrial evidence, particularly in East Antarctica, due to the limited number of coastal mountain ice-free regions and their lack of datable material, particularly for radiocarbon dating. In parallel with these modelling uncertainties, reductions in the calculated volumes of the Laurentide and Fennoscandian ice caps appear to account for only a portion of the observed ~120 m rise in global sea level since LGM times.

In the absence of any direct and/or local evidence for the volume of ice in Antarctica at the global LGM, early estimates were mostly based on the difference between known sea level change, and the known (Northern Hemisphere) ice sheets (Nakada & Lambeck 1988). As more direct evidence from the continent becomes increasingly available, estimates of the volume of grounded ice in Antarctica at the LGM are becoming correspondingly much smaller, particularly in East Antarctica. While it is clear from grounding line studies (Conway *et al*. 1999) that there were significant expansions of the West Antarctic Ice Sheet (WAIS) in the Ross Sea region, investigations on the main East Antarctic Ice Sheet (EAIS) have indicated relatively small ice sheet increases during the LGM (Gore *et al*. 2001, Mackintosh *et al*. 2007). Similarly, isostatic rebound along the McMurdo Sound coast based on

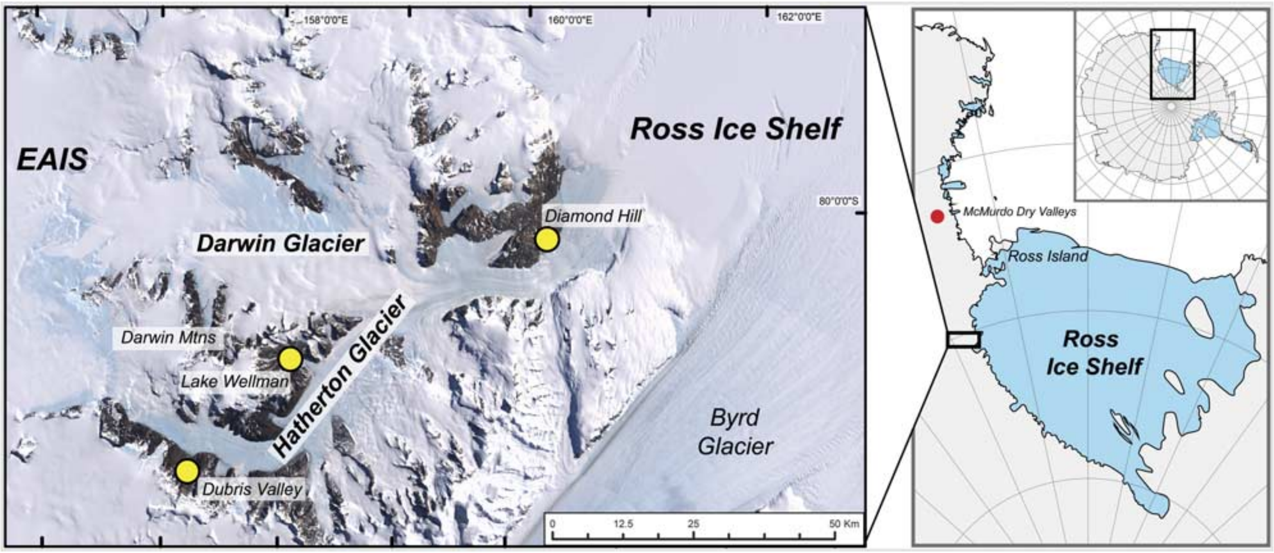

Fig. 1. Regional map (left figure) showing the location of Lake Wellman within the Hatherton and Darwin glacial system which discharges into the Ross Ice Shelf. Inset (right figure) shows location of Hatherton Glacier region (small black rectangle) with respect to Dry Valleys region of the Transantarctic Mountains (red dot). Diamond Hill and Dubris Valley are other field sites targeted for cosmogenic exposure dating.

raised beach elevations (Butler 1999) suggest minimal isostatic loading during the same period.

This paper provides new geological evidence of ice sheet extent and thickness over at least the past few hundred thousand, and perhaps the past two million years within a sector of the Transantarctic Mountains in order to better constrain computer model estimates of palaeo-ice sheet changes. We describe the glacial history based on new *in situ* cosmogenic nuclide exposure ages of an ice-free region in the Darwin Mountains on the edge of the Hatherton Glacier, referred to as the Lake Wellman area (Fig. 1). The location is one of the study sites along the Latitudinal Gradient Project of the Transantarctic Mountains (Howard-Williams *et al.* 2006). The set of 25 cosmogenic exposure ages of erratics collected along two altitudinal transects allows estimates of ice volume changes of the Hatherton Glacier which, at the spatial resolution examined here, constrains ice sheet models and provides input into the biogeographic and evolutionary history of the Darwin Mountains region. Previous work from the Lake Wellman area of the Transantarctic Mountains has been used to support a "big ice" view of Antarctic glacial expansion at the LGM (Denton & Hughes 2002). Our results have strong implications for the role of the Ross Ice Shelf in ice sheet volume calculations at the LGM.

The Lake Wellman area

The Hatherton Glacier flows from the EAIS into the lower Darwin Glacier, which in turn discharges ice into the Ross Ice Shelf (Fig. 1). The Darwin–Hatherton system is an important outflow glacier system that connected the East and West Antarctic ice sheets during previous glacial maxima. The advance and retreat of the Hatherton is recorded in well-preserved glacial moraines that are found in numerous side entrant valleys of the Darwin Mountains along the length of the glacier. Ice-free cirques and valleys in the Darwin Mountains are cut into Palaeozoic sandstones of the Beacon Supergroup and thick dolerite sills of the Jurassic Ferrar Supergroup (Haskell *et al.* 1964). In the vicinity of Lake Wellman, a large currently ice-free area had previously been completely or partially covered by ice (Bockheim *et al.* 1989) resulting in multiple drift sheets deposited by palaeo-advances of the Hatherton Glacier. These deposits were mapped in the late 1970s by Bockheim *et al.* (1989) who identified five drift sheets that occur discontinuously in the ice-free regions extending over an elevation range of about 800 m from the edge of Lake Wellman, which is at 845 m above sea level (m a.s.l.) (Fig. 2). From youngest to oldest, with increasing distance from the present day margins of Lake Wellman, these are: 1) Hatherton, 2) Britannia I, 3) Britannia II, 4) Danum, and 5) Isca.

Currently, the altitude of the ice surface of the Hatherton Glacier at midstream is 960 m a.s.l. Bockheim *et al.* (1989) estimated the upper limit of the Hatherton drift to have been 20–70 m above the present surface of Lake Wellman, the Britannia drift to extend a further 450 m above the Hatherton, and the Danum to be 50–100 m above the Britannia drift limit. This effectively suggested that the total ice thickening at the time of deposition of the Danum drift sheet was about 600 m higher than the current elevation defined by Lake Wellman and given a modern Hatherton ice surface altitude of 960 m a.s.l., an ice thickness of at least 500 m greater than today. The drift sheets are described as lithologically uniform dominated by dolerite and sandstone boulders of variable size and shape

https://doi.org/10.1017/S0954102010000799 Published online by Cambridge University Press

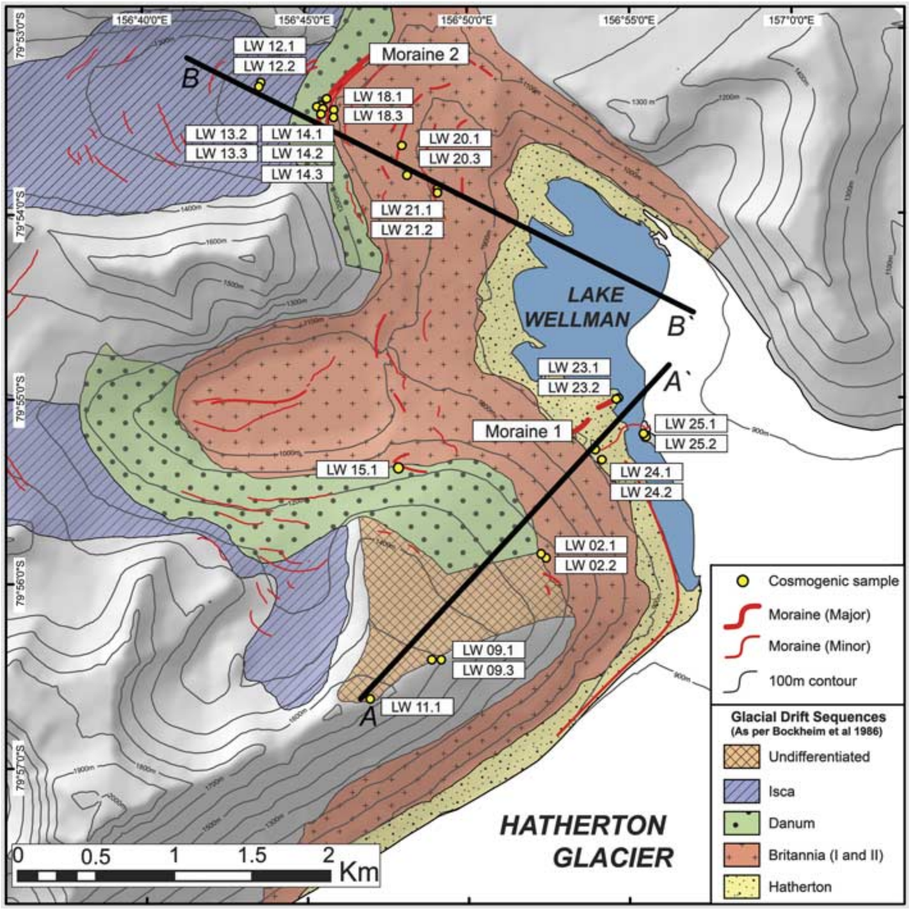

Fig. 2. A geomorphological map of the Lake Wellman area showing the distribution of the four main drift sequences after Bockheim *et al*. (1989). Black bold lines A–A' and B–B' represent altitudinal transects along which samples were collected from glacial deposits for exposure age dating. Sample sites are designated by rectangular boxes labelled as LW xx. Aerial photographs of moraines 1 and 2 are shown in Fig. 4. Hatherton Glacier ice flows from bottom-left to top-right in a direction semi-parallel to transect A–A'.

(Fig. 3) in unconsolidated gravel and sandy matrix. There are a few granitic erratics that have been transported into the area by ice; granite does not crop out locally in the Darwin Mountains. Prominent moraine ridges and boulder lines both separate and occur within the drift sheets (Fig. 2). Individual drift sheets show increasingly poor morphological preservation with distance (i.e. age) from the current ice surface. The percentage of surface modified boulders (varnished, fractured,

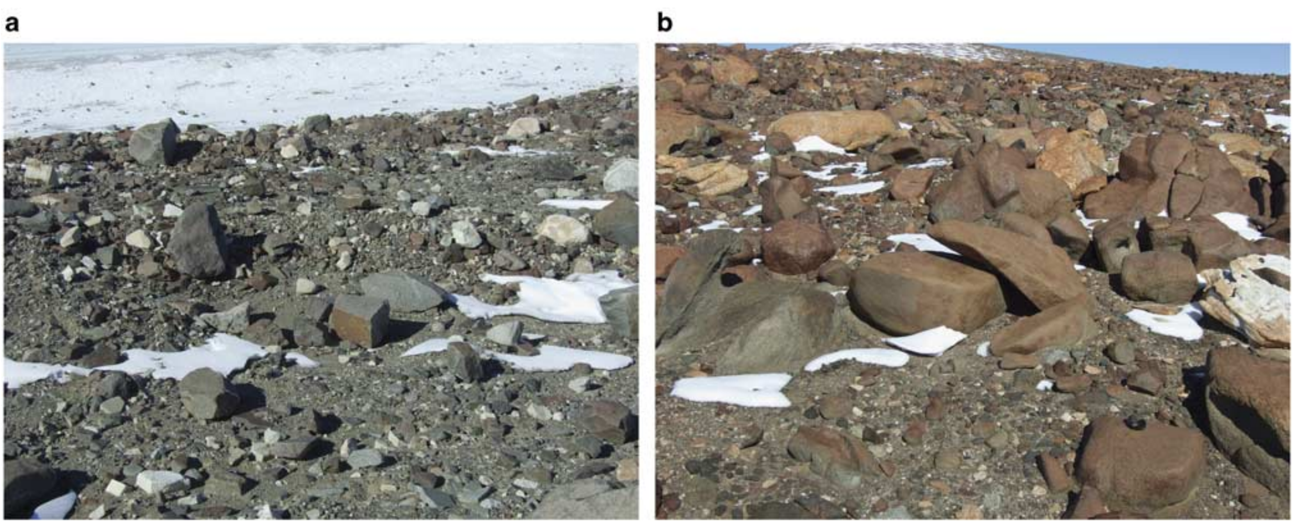

Fig. 3. Photographs showing the surface characteristics of **a.** the Hatherton, and **b.** the Isca drifts. The older Isca drift shows extensive surface weathering and desert tarnish whereas the younger Hatherton drift shows minimal weathering, glacial striations and more angular debris.

https://doi.org/10.1017/S0954102010000799 Published online by Cambridge University Press

a b

Fig. 4. Photographs showing the main features of **a.** Moraine 1 on the Hatherton drift, and **b.** Moraine 2 at the boundary of the Britannia and Danum drifts.

pitted, and spalled) increases progressively from the Hatherton to the Isca drifts. The varnishing and cavernous weathering (tafoni) also increases with age. Perched, striated and plucked boulders are more common in the younger drift sheets, particularly the Hatherton and Britannia drifts. The Hatherton drift has prominent moraine ridges (Fig. 4, marked as Moraine 1 on Fig. 2) and ice-cored hummocky terrain. A prominent moraine ridge separates the Britannia and Danum drifts (Fig. 4, see Moraine 2 on Fig. 2). This ridge has an asymmetric profile, is 1130 m long, 11 m high and 6 m wide and is made up of angular to sub-rounded moderately weathered clast-supported sandstone and dolerite boulders with rare granite clasts. The boundary between the Danum and the oldest drift, Isca, is not obvious in the Lake Wellman area, and in addition, in the Lake Wellman area it is not possible to distinguish the Britannia I from the Britannia II drift. Bockheim *et al.* (1989) concluded they were part of the same major glaciation event even though they were distinguishable in other locations.

Age of drift sheets

Bockheim *et al.* (1989) used ^{14}C dating of blue green algae among and beneath surface clasts on the Hatherton and Britannia drift surfaces to provide minimum ages for glacial recession. On the assumption that these algae grew in former lakes or ponds on the drift surfaces and that they had been preserved since the last glacial retreat, Bockheim *et al.* (1989) concluded that ice retreated from its maximum advance position on the Britannia drift prior to 9420–10 250 cal yr BP, that the Hatherton drift is older than 5270 cal yr BP and that the ice was near its present configuration by 5740–6020 cal yr BP. These radiocarbon ages have been used by Conway *et al.* (1999) to suggest that the WAIS damned the entrance to the Darwin–Hatherton glacial system during Britannia times (i.e. prior to ~10 ka) and that the Hatherton drift was deposited when its grounding line retreated further southward than the junction between the Darwin Glacier and the Ross Ice Shelf at about 6 ka, allowing the floating Ross Ice Shelf to fill the volume vacated by the receding WAIS. From correlations with drift in the McMurdo Sound region and from the local ^{14}C ages, Bockheim *et al.* (1989) assigned an early Holocene age for the Hatherton drift, a LGM age for the Britannia drift and marine isotope stage (MIS) 6 for the Danum drift (140–160 ka). They correlate Britannia drift with the Ross Sea drift representing the limit of ice at the LGM.

As pointed out by Bockheim *et al.* (1989), radiocarbon ages of these algae deposits can only provide a minimum age for the drifts as the algae grow in seasonally wet depressions and lakes on the glacial landforms after ice evacuation. In the Dry Valleys of southern Victoria Land, the inference of a direct relationship between the recession of the ice and the growth of the algae is supported by the geomorphological context of moraine impoundment of lakes (Sugden *et al.* 2006). In the Darwin area, however, the geomorphological context is much less certain and the algal ages reflect the onset of the availability of seasonal water rather than necessarily, ice retreat. Moreover, there is no means by which to determine the long-term preservation of algae. Clearly, to quantify the scale of ice sheet advance, its timing and the embedded phenomenon of glacial refugia, a more secure and reliable method is required to determine the age of the drift sheets. In this setting, only surface exposure dating (SED) using *in situ* cosmogenic radionuclides (CRN) ^{10}Be and ^{26}Al provides the opportunity to directly date glacial features.

Sampling and analyses

The area was remapped from satellite images and extensively ground truthed using the map of Bockheim *et al.* (1989)

Table I. Sample and site description for samples from Lake Wellman, Hatherton Glacier in the Darwin Mountains, Antarctica.

Sample name	Glacial drift sequence (1)	Location		Elevation (m)		Sample type	Sample dimensions (cm)	Thickness (cm)	Topographic Shielding (3)
		Latitude (S)	Longitude (E)	a.s.l.	above Lake Wellman (2)				
Transect A									
LW 11.1	Isca	79°56'41.594	156°46'32.068	1646	801	Granite	174 x 105 x 84	5.0	0.995
LW 09.1	Isca	79°56'25.702	156°49'10.135	1501	656	Sandstone	256 x 290 x 130	5.0	0.995
LW 09.3	Isca	79°56'25.675	156°48'52.191	1508	663	Granite	130 x 170 x 45	1.5	0.995
LW 02.1	Britannia	79°55'53.771	156°52'17.670	1246	401	Granite	800 x 500 x 300	6.0	0.995
LW 02.2	Britannia	79°55'53.774	156°52'16.794	1237	392	Sandstone	12 x 12 x 10	10.0	0.995
LW 15.1	Danum	79°55'19.236	156°47'54.995	1136	291	Sandstone	105 x 156 x 185	4.0	0.985
LW 24.1	Hatherton	79°55'20.608	156°54'07.684	895	50	Granite	115 x 160 x 50	5.0	0.995
LW 24.2	Hatherton	79°55'17.811	156°53'57.691	892	47	Granite	86 x 93 x 52	3.0	0.995
LW 23.1	Moraine 1	79°55'00.826	156°54'39.387	852	7	Sandstone	33 x 18 x 14	3.0	0.995
LW 23.2	Moraine 1	79°55'01.111	156°54'35.643	850	5	Granite	12 x 8 x 5	5.0	0.995
LW 25.1	Hatherton	79°55'12.344	156°55'25.965	852	7	Granite	125 x 86 x 44	5.0	0.995
LW 25.2	Hatherton	79°55'13.445	156°55'30.546	845	0	Sandstone	125 x 96 x 45	5.0	0.995
Transect B									
LW 12.1	Isca	79°53'19.798	156°43'53.586	1150	305	Sandstone	174 x 105 x 84	1.0	0.990
LW 12.2	Isca	79°53'19.785	156°43'52.768	1155	310	Granite	180 x 212 x 84	6.0	0.990
LW 13.2	Danum	79°53'25.813	156°45'26.798	1107	262	Sandstone	180 x 211 x 103	5.0	0.995
LW 13.3	Danum	79°53'25.933	156°45'22.423	1112	267	Granite	158 x 157 x 93	2.5	0.995
LW 14.1	Moraine 2	79°53'26.403	156°45'33.541	1119	274	Sandstone	10 x 6 x 8	5.0	0.995
LW 14.2	Moraine 2	79°53'26.546	156°45'33.807	1115	270	Sandstone	24 x 60 x 51	5.0	0.995
LW 14.3	Moraine 2	79°53'26.629	156°45'33.400	1115	270	Sandstone	17 x 17 x 8	5.0	0.995
LW 18.1	Britannia	79°53'26.942	156°45'54.120	1087	242	Sandstone	290 x 177 x 203	5.0	0.990
LW 18.3	Britannia	79°53'29.376	156°45'53.633	1101	256	Granite	180 x 83 x 110	5.0	0.990
LW 20.1	Britannia	79°53'38.668	156°47'59.290	1018	173	Sandstone	220 x 177 x 106	3.0	0.995
LW 20.3	Britannia	79°53'48.224	156°48'09.117	1025	180	Granite	150 x 110 x 60	3.0	0.995
LW 21.1	Britannia	79°53'52.584	156°49'06.008	981	136	Granite	74 x 93 x 84	2.5	0.995
LW 21.2	Britannia	79°53'53.970	156°49'05.287	982	137	Sandstone	177 x 78 x 56	2.5	0.995

(1) Associated drift sequence nomenclature according to Bockheim *et al*. (1989)
(2) Lake Wellman is at 845 m a.s.l. equivalent to the lowest altitude sample, LW 25.2. The altitude of the modern ice surface of Hatherton Glacier is defined as 960 m a.s.l.
(3) Attenuation length = 150 g cm^2, rock density = 2.7 g cm^3

as a base. The morphology and sedimentology of the drifts and moraines were closely examined with a particular focus on the SED sample sites. We collected glacially transported sandstone and granitic erratics exposed sub-aerially on the upper surfaces of the four drifts described above from the Lake Wellman area to determine *in situ* ^{10}Be and ^{26}Al cosmogenic exposure ages. The samples came from two elevation transects, from modern ice surface to the highest altitude glacial drift (Fig. 2). Transect A–A' includes erratics from the intersection of the modern day ice surface, from the Hatherton (including Moraine ridge 1), Britannia and Isca drifts, whilst transect B–B' covers erratics from the Britannia drift, the prominent Moraine ridge 2, Danum and Isca drifts. Stable, rounded sandstone and granite clasts, in open sky settings, were preferentially sampled because they demonstrate glacial transport, minimize the likelihood of inheritance and are less likely to have moved since deposition. Samples that (to the best of our knowledge) exhibited signs of post-depositional re-orientation or partial burial by sediment or periglacial weathering were avoided. In some cases, small erratics perched on larger stable boulders were sampled. Table I gives locations and descriptions of those erratics selected for dating.

In order to supplement SED sampling data, sedimentological characteristics were compiled for the area around the sample sites. This was achieved using a 50 m transect at each general sampling location with individual clasts sampled at 1 m intervals along the transect (i.e. $n = 50$) for lithology, angularity, size and weathering characteristics (a full dataset is presented in Hood 2010). For 'drift' samples, transects were run parallel to the slope so that each transect represented a discrete elevation. For moraines, transects were taken from the crest and followed the trend of the crest line. A summary of lithology and angularity data are presented in Figs 5 & 6. Dolerite is the modal lithology in all samples, with lesser percentages of gabbro, granite, sandstone, basalt and gneiss. While there is no definitive trend with elevation the following two points should be noted. Firstly, Ferrar Dolerite and Beacon Supergroup sandstones are, or at least could be, of local provenance, but all samples contain lithologies (notably granite) that do not crop out in the Lake Wellman area. Secondly, while lithologies are not systematically different,

https://doi.org/10.1017/S0954102010000799 Published online by Cambridge University Press

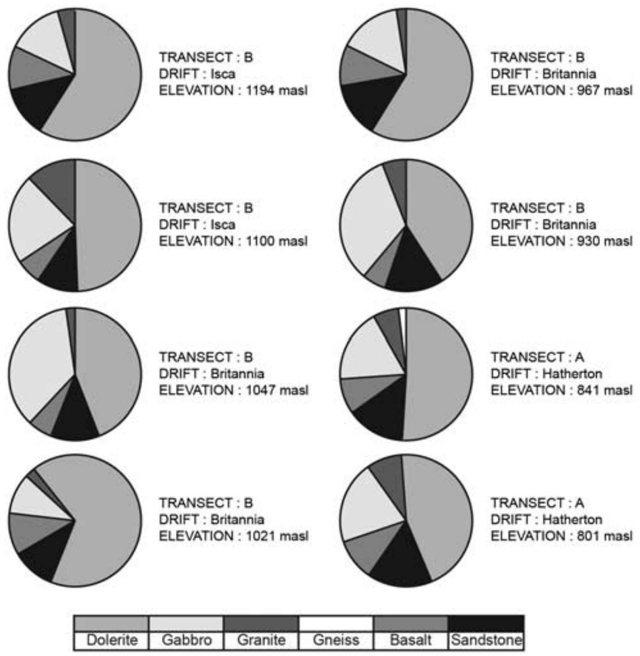

Fig. 5. Pie diagrams showing the proportion of different lithologies within the glacial drifts at different elevations within the Lake Wellman area.

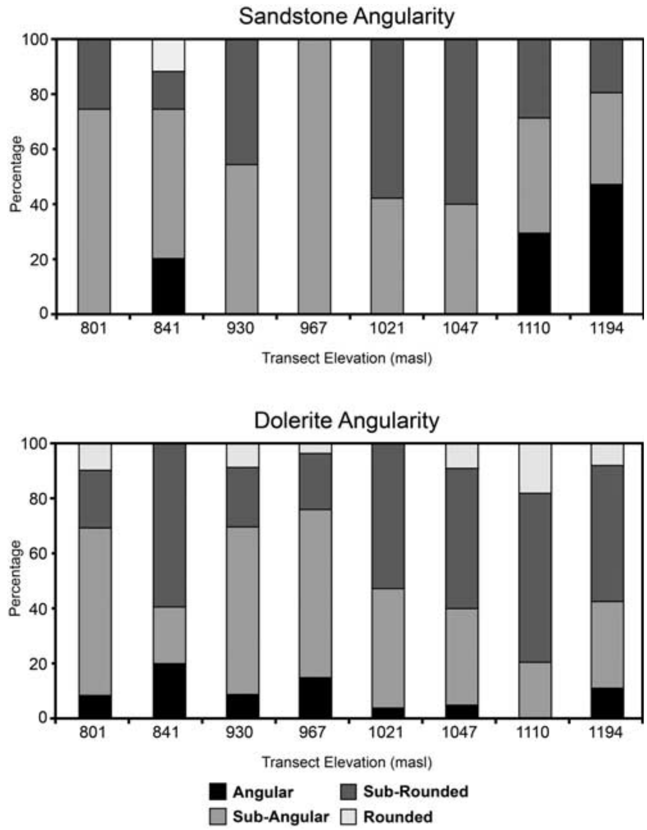

Fig. 6. Angularity histograms for dolerite and sandstone clasts within the glacial drifts in the Lake Wellman area.

some of the other characteristics are. Angularity measurements based on the 6-point Power's index indicate that there are differences between lower elevation samples and higher elevation samples. The angularity measurements need to be compared within, rather than between, lithologies and consequently only for dolerite are sample sizes statistically valid. For dolerite, the samples can be delineated into more rounded material above 1000 m and less rounded below (Fig. 6). For sandstones, the same trend is replicated, though even more strongly, and a further sub-division of the samples from above 1100 m with those from 1000–1100 m is suggested (Fig. 6).

Exposure age measurements and calculations

Cosmogenic targets for ^{10}Be and ^{26}Al were prepared at the University of Canterbury preparation laboratory following protocols and procedures provided by the Australian Nuclear Science and Technology Organisation (ANSTO) (Child *et al.* 2000). Once processed, ^{10}Be and ^{26}Al concentrations were measured in 25 quartz samples at the ANTARES Accelerator Mass Spectrometer (AMS) facility at ANSTO (Fink & Smith 2007). Table II gives the results of all the AMS measurements and Table III the calculated exposure ages.

Each set of eight unknown samples were processed with full chemistry procedural blanks for ^{10}Be and for ^{26}Al prepared from commercially purchased 1000 ppm ICP standard Be and Al solutions. The mean ^{10}Be/^{9}Be chemistry blank was 34.6 ± 5.0 (1σ) x 10^{-15} ($n = 6$, 3 targets) and mean ^{26}Al/^{27}Al chemistry blank was 27.8 ± 14.0 (1σ) x 10^{-15} ($n = 4$, 2 targets). The same 1000 ppm ICP Be solution was used as carrier for ^{10}Be samples. Aluminium concentrations in purified quartz solutions were measured by ICP-OES with a representative uncertainty of ± 4%. Reproducibility of native Al assay in duplicate solutions were < 2% for all samples. Apart from three of the 25 samples measured, final AMS ratios after normalization to standard reference materials ranged from 606 to 52 060 x 10^{-15} for ^{10}Be/^{9}Be and from 297 to 183 150 x 10^{-15} for ^{26}Al/^{27}Al. Total analytical errors for ^{10}Be concentrations (atoms per gram quartz) ranged from 0.9% to 4.5% and for ^{26}Al concentrations from 1.5% to 9.0%. Three samples gave very low AMS ratios - these were LW 23.1, LW 24.2 and LW 25.1 with ^{10}Be /Be ratios of (26 ± 4, 122 ± 7 and 44 ± 5) x 10^{-15} respectively, and ^{26}Al/Al ratios of (19 ± 10, 224 ± 31 and 43 ± 16) x 10^{-15}, respectively.

Given the relatively large spread in both ^{10}Be/^{9}Be and ^{26}Al/^{27}Al ratios (about 10^3), care was taken to asses ion-source cross-contamination by frequent measurement of cathodes loaded with Nb metal powder which was used as a mixing agent for the Be and Al oxide powders. Independent repeat AMS measurements per sample were combined as weighted means selecting the larger of the mean standard error or total statistical error. The final analytical error

Table II. Results of AMS measurement for ^{10}Be and ^{26}Al for the Lake Wellman samples.

Sample name	$^{10}Be/^{9}Be$ ratio (x 10^{-15}) (1)	$^{10}Be/^{9}Be$ error (x 10^{-15}) (2)	$^{26}Al/^{27}Al$ ratio (x 10^{-15}) (3)	$^{26}Al/^{27}Al$ error (x 10^{-15}) (2)	Quartz mass (g)	^{9}Be carrier mass (mg)	Al concentration (ppm)
Transect A							
LW 11.1	31 726	338	129 332	2422	50.20	0.4043	n.a.
LW 09.1	48 356	665	20 005	540	51.06	0.4404	270
LW 09.3	52 066	655	183 145	2771	50.13	0.4087	n.a.
LW 02.1	3467	28	2108	84	75.09	0.4097	304
LW 02.2	1010	60	383.0	40	76.55	0.4042	313
LW 15.1	22 282	510	8484	251	75.49	0.4153	211
LW 24.1	2982	39	7944	167	100.05	0.3989	23
LW 24.2	122.4	6.5	223.8	31.0	99.85	0.3998	27
LW 23.1	26.4	3.9	18.9	10.0	99.97	0.5157	236
LW 23.2	762.8	13.5	1002	47	92.35	0.4064	57
LW 25.1	44.0	5.0	43.2	16.3	100.24	0.4107	62
LW 25.2	605.9	12.1	296.9	26.0	93.95	0.4028	193
Transect B							
LW 12.1	5405	246	2183	88	76.19	0.4048	233
LW 12.2	14 867	136	16 646	460	75.22	0.4133	80
LW 13.2	3121	87	838	40	75.21	0.4018	395
LW 13.3	9164	81	26 986	660	75.22	0.4017	25
LW 14.1	4195	52	n.a.		45.38	0.4440	n.a.
LW 14.2	18 775	204	8095	357	89.63	0.3991	125
LW 14.3	374.6	33.0	n.a.		44.95	0.4310	n.a.
LW 18.1	1877	30	1741	157	87.91	0.4065	92
LW 18.3	9465	114	13 661	628	100.23	0.4058	57
LW 20.1	2407	65	984	46	108.40	0.4038	193
LW 20.3	1942	27	1330	69	100.38	0.4104	109
LW 21.1	1703	56	696	62	100.05	0.4037	196
LW 21.2	1501	24	662	42	104.85	0.4133	190

(1) Measured against NIST SRM-4325 with a nominal value of 27 900 x 10^{-15}. Final AMS ratio from weighted mean of repeat measurements.
(2) The quoted 1σ error is the larger of total statistical error or weighted error in mean. Additional 2% (1σ) error added in quadrature based on reproducibility of AMS standard measurements.
(3) Measured against SRM PRIME-Z93-0221 with a nominal value of 16 800 x 10^{-15}.

includes (in quadrature) a 2% systematic variability in repeat measurement of AMS standards (Fink & Smith 2007). Nishiizumi *et al*. (2007) have recently presented revised nominal values of $^{10}Be/^{9}Be$ isotopic ratios for AMS standard reference materials (SRMs) which resulted in a 1.106 ± 0.012 factor reduction in their previously accepted nominal ratios. This in turn mandates corresponding reductions in sea level high latitude (SLHL) spallation calibration scaling factors (summarized in table 6 of Balco *et al*. (2008) for various scaling models). Similarly, we apply the same 10.6% reduction in the value of the AMS SRM for ^{10}Be, NIST-4325, in use at the ANTARES AMS Facility (Fink & Smith 2007). AMS ^{10}Be concentrations presented in this work are normalized to NIST-4325 with a revised nominal $^{10}Be/^{9}Be$ value of 27 900 ± 300 x 10^{-15}, and ^{10}Be exposure ages are calibrated with a SLHL production rate based on Stone-Lal scaling methods (Stone 2000) reduced from 5.10 (including a 2.5% muon component production) to 4.60 atoms/g/yr. Final ^{26}Al concentrations are normalized to AMS SRM PRIME-Z93-0221, with a nominal $^{26}Al/^{27}Al$ value of 16 800 x 10^{-15}. ^{26}Al exposure ages are calibrated with a SLHL production rate based on Stone-Lal scaling methods (Stone 2000) of 30.7 atoms/g/yr (including a 2.5% muon component production). Errors of 10% are assigned to both the ^{10}Be and ^{26}Al SLHL production rates which are propagated in quadrature with the total analytical AMS errors in cosmogenic concentrations. We use the new published ^{10}Be half-life (Korschinek *et al*. 2009) of 1.387 ± 0.012 Ma and an ^{26}Al half-life of 0.70 Ma.

Corrections to site specific production rates due to horizon topographic shielding of cosmic rays were no larger than 1% and negligible. Sample thicknesses ranged from 1.5–6 cm. Thickness corrections were carried out by integrating the effective flux over the sample thickness resulting in a maximum correction of 0.950 (using $\Lambda = 150\,g\,cm^2$ and $\rho = 2.7\,g\,cm^3$). Corrections for seasonal snow cover or erosion of boulder surface were not included.

Results and discussion

Interpreting exposure ages of erratics

The application of cosmogenic exposure dating in regions where ice sheets are the principal agent of bedrock sculpting and transport of erratics, requires an appreciation

https://doi.org/10.1017/S0954102010000799 Published online by Cambridge University Press

Table III. ^{10}Be and ^{26}Al cosmogenic exposure ages based on zero erosion.

Sample name	Glacial drift sequence	^{10}Be (atoms g^{-1}) (x 10^3)	^{10}Be error (atoms g^{-1}) (x 10^3)	^{26}Al (atoms g^{-1}) (x 10^3)	^{26}Al error (atoms g^{-1}) (x 10^3) (1)	Minimum ^{10}Be exposure age (ka) (2)	Exposure age error (ka) (3)	Minimum ^{26}Al exposure age (ka) (4)	Exposure age error (ka) (3)	$^{26}Al/^{10}Be$ ratio	$^{26}Al/^{10}Be$ error
Transect A											
LW 11.1	Isca	17 077	423	n.a.		929	103	n.a.		n.a.	
LW 09.1	Isca	27 874	732	120 356	6400	2275	345	1978	474	4.32	0.26
LW 09.3	Isca	28 369	728	n.a.		2196	356	n.a.		n.a.	
LW 02.1	Britannia	1264	30	14 307	870	78.1	7.0	137	15	11.32	0.74
LW 02.2	Britannia	356.3	22.7	2678	310	22.6	2.3	25.3	3.4	7.52	0.98
LW 15.1	Danum	8192	262	39 895	2180	630	66	491	62	4.87	0.31
LW 24.1	Hatherton	794.6	20.6	4128	210	65.5	6.0	50.8	5.1	5.20	0.29
LW 24.2	Hatherton	32.8	1.9	136.7	20.0	2.6	0.3	1.6	0.3	4.17	0.65
LW 23.1	Moraine 1	9.1	1.4	100.1	50.0	0.8	0.1	1.2	0.6	10.99	6.03
LW 23.2	Moraine 1	224.3	6.4	1281	80	19.1	1.7	16.2	1.7	5.71	0.41
LW 25.1	Hatherton	12.0	1.4	59.8	10.0	1.0	0.2	0.7	0.3	4.97	1.31
LW 25.2	Hatherton	173.6	5.2	1279	130	14.8	1.3	16.2	2.1	7.36	0.76
Transect B											
LW 12.1	Isca	1919	97	11 335	690	128	13	115	13	5.91	0.47
LW 12.2	Isca	5460	132	29 708	1590	395	38	340	39	5.44	0.32
LW 13.2	Danum	1114	40	7389	490	76.7	7.2	76.6	8.4	6.63	0.50
LW 13.3	Danum	3271	79	14 975	780	227	22	157	17	4.58	0.26
LW 14.1	Moraine 2	2743	70	n.a.		192	18	n.a.		n.a.	
LW 14.2	Moraine 2	5587	139	22 671	1440	415	41	254	30	4.06	0.28
LW 14.3	Moraine 2	240.1	21.8	n.a.		16.1	2.0	n.a.		n.a.	
LW 18.1	Britannia	580.2	16.0	3571	360	40.4	3.7	37.1	4.9	6.16	0.65
LW 18.3	Britannia	2561	65	17 300	1120	183	17	192	22	6.75	0.47
LW 20.1	Britannia	599.1	21.0	4242	280	43.3	4.1	45.9	5.1	7.08	0.53
LW 20.3	Britannia	530.6	14.0	3221	220	38.1	3.5	34.5	3.9	6.07	0.45
LW 21.1	Britannia	459.2	18.0	3046	300	34.1	3.3	33.7	4.5	6.63	0.71
LW 21.2	Britannia	395.5	11.0	2807	220	29.3	2.7	31.0	3.7	7.10	0.59

(1) Error in ^{26}Al concentration includes a 4% error in ICP-OES measurement of Al concentration in quartz mass.
(2) ^{10}Be decay constant = 5.00×10^{-7} ($t_{\frac{1}{2}}$ = 1.387 Ma), ^{10}Be production rate = 4.60 +/- 0.42 atoms/g/year (see text for details).
(3) Age error includes a 9% standard error in sea level high latitude production rate in quadrature with total analytical AMS error.
(4) ^{26}Al decay constant = 9.90×10^{-7} ($t_{\frac{1}{2}}$ = 0.70 Ma), ^{26}Al production rate = 30.7 +/- 2.8 atoms/g/year.

of the various factors which can modify the cosmic ray exposure dose of a transported boulder following deposition on an exposed bedrock surface following ice retreat (Sugden *et al*. 2005). These factors address the assumption that the measured radionuclide concentration directly reflects simple and continuous exposure. Given the higher likelihood of cold-based ice activity in the Polar Regions, it is not uncommon to observe young erratics perched on ancient bedrock surfaces (Briner *et al*. 2003). The near-absence of sub glacial bedrock erosion due to non-sliding cold-based ice allows long-term accumulation and partial preservation of cosmogenic nuclide inventories from previous exposures. The most recent advance may well deposit entrained erratics with minimal inheritance, yet not erode sub-glacially or alter previously deposited moraines (Miller *et al*. 2002, Stroeven *et al*. 2002, Fabel *et al*. 2006). The observational evidence for cold-based ice overriding can be as subtle as minor differences in the degree of surface weathering across subdued demarcation trim lines (Sugden *et al*. 2005).

In other Antarctic studies, erratic and bedrock exposure ages as a function of altitude from ice edge to mountain peak (Stone *et al*. 2003, Mackintosh *et al*. 2007, Lilly *et al*. 2010) have become an effective method to estimate local ice volume of the most recent advance. Nunataks protruding today through the ice sheet can thus act as 'dipsticks' of historic ice thickness. In the absence of inheritance, these exposure ages should trace out a monotonic relationship of increasing age with altitude. The prevalence of a varying and unknown component of inheritance in the cosmogenic nuclide inventory often negates such a simplistic expectation, as recycled erratics or those freshly plucked from bedrock can be re-deposited with an inheritance signal and may not always represent exposure since last ice advance. This forces a working hypothesis to be that the youngest erratic age at the highest elevation best represents minimum (or zero) inheritance and hence the limit of the most recent advance (Bentley *et al*. 2006, Mackintosh *et al*. 2007). Unfortunately, such a scheme requires judicious and multiple sampling. Stone *et al*. (2003) in attempting to map Holocene ice volume profiles in Marie Byrd Land, Antarctica, provided 10 erratic ages from Mount Rea over an elevation span from 610 to

780 m a.s.l., to be confronted with exposure ages ranging from 10.4–112 ka showing no correlation to elevation. The single erratic with the lowest exposure age (10.4 ka) at 715 m was deemed as the best choice to locate early Holocene ice elevation for comparison to late Holocene ages at lower altitudes at other coastal nunataks. This example highlights the complexity of exposure dating in environments where transported debris can be recycled and partially preserved over repetitive glaciations.

In some cases, the sampling of erratic-bedrock pairs can provide information not only on timing of the last advance but also on the degree to which the locality is affected by passage of cold-based ice. Alternatively, the processes of moraine stabilization, post-depositional re-orientation or long-term debris cover will generate apparent young exposure ages (Gosse & Phillips 2001, Putkonen & Swanson 2003, Briner *et al*. 2005). If this process dominates the geomorphological glacial landscape, then selecting the older exposure ages may be more representative of ice advance than selecting the youngest exposure ages if inheritance dominates. In addition, the measurement of a ^{26}Al concentration paired with ^{10}Be in the same quartz sample allows determination of a ^{26}Al/^{10}Be ratio. Non-concordant ages between these two isotopic systems, as demonstrated by plots of ^{26}Al/^{10}Be ratios versus ^{10}Be, can then be used to identify samples which exhibit extensive burial histories (or more specifically, pre-irradiation followed by burial and then re-exposure). Although such identification requires burial histories in excess of 150–200 ka, it at least can qualify the *a priori* use of a sample's ^{10}Be exposure age as reflecting continuous exposure. It is important to note that a subset of recycled samples which have concordant isotope ages (within the usual error criteria of 2σ overlap), and thus would be classified as those with a "continuous exposure" (i.e. have not undergone a 3-stage exposure history), may well have an inheritance component. For these samples, both the ^{26}Al and ^{10}Be age would fall outside acceptable error limits of the mean moraine age based on the majority of other moraine samples. However, in the absence of a corresponding ^{26}Al age, ^{10}Be ages which lie more than 2σ or 3σ above the mean population age for a given glacial feature, will always carry some uncertainty as to its reliability and basis for rejection. A similarly 'deviant' ^{26}Al age in the same sample verifies the erratic as an outlier but more so, provides sound justification for removing the sample from the averaging process.

Only a limited number of Antarctic glacial studies provide ^{26}Al-^{10}Be exposure age pairs (Bentley *et al*. 2006, Fink *et al*. 2006, Mackintosh *et al*. 2007, Lilly *et al*. 2010). This has more to do with the fact that the large majority of cosmogenic studies in Antarctica have focussed on its LGM ice history making ^{26}Al measurements rather ineffective as an indicator of burial in comparison to increasing the population of ^{10}Be samples. Moreover, due to technical aspects, it is difficult in young aged samples to achieve the required statistical precision in the ^{26}Al/^{10}Be ratio to identify burial. These considerations with respect to ^{26}Al ages become far more relevant and beneficial when exposure ages exceed ~ 100 ka, because both the total error in the ^{26}Al/^{10}Be ratio decreases and burial histories and boulder recycling are more likely in older samples. An added complication within this work relates to the absence of minimally modified glaciated bedrock surfaces to allow bedrock-erratic pairs to be collected. The Lake Wellman area is dominated by a carpet of extensive and thick diamict in the form of drift sheets containing sub-angular clasts and boulders of varying dimensions, orientations and with varying degrees of weathering. The few prominent unconsolidated moraines overlie drift sheets that are discontinuous, making sample selection all the more difficult. In the absence of erratics on bedrock, the next level of choice were large, blocky and flat-surfaced erratics however there remains the uncertainty of exhumation, drift stabilization and freeze-thaw as a further factor driving exposure ages younger. In this study we attempt to apply these various approaches in evaluating and interpreting zero-erosion model exposure ages for ^{10}Be and ^{26}Al with due concern for the complexities of the glacial geomorphology inherent in polar studies using cosmogenic isotopes for dating. The zero erosion model applied to the assumption that the analysed samples have experienced no erosion.

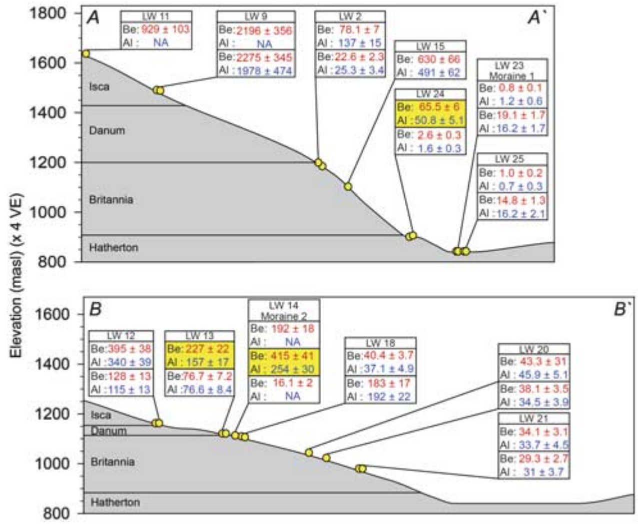

Fig. 7. Elevation versus ^{10}Be and ^{26}Al exposure ages for analysed samples from transect A-A' and B-B'. All ages are given in ka. Red numbers represent ^{10}Be ages and blue ^{26}Al ages. Yellow boxes indicate samples that reflect a burial history.

Exposure age results

Transect A–A' ^{10}Be exposure ages ranged from 0.8–2275 ka, and from 16–415 ka for transect B–B'. Corresponding ^{26}Al ages for A–A' ranged from 0.7–1978 and from 31–340 for B–B'. For four samples (LW 11.1, LW 9.3 on transect A–A';

https://doi.org/10.1017/S0954102010000799 Published online by Cambridge University Press

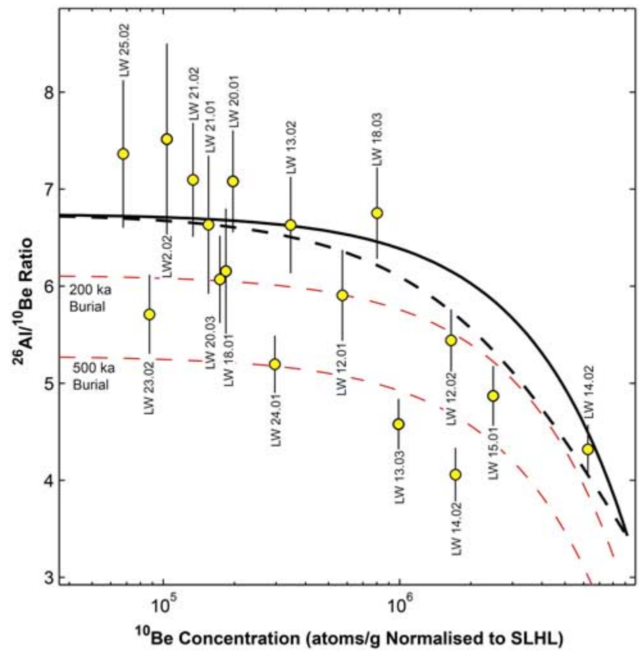

Fig. 8. A plot of $^{26}Al/^{10}Be$ ratios versus normalized SLHL ^{10}Be concentrations showing the exposure history of analysed samples The upper bold black curve represents continuous exposure at zero erosion, the lower dashed black curve steady state erosion. Exposed surface samples undergoing erosion will fall within the two loci defining an area termed the steady state exposure-erosion island. Burial isochrons of 200 ka (red thin red curve) and 500 ka (dashed red curve) are also shown. Error bars are derived from analytical errors only. Error envelopes for the exposure-erosion island (based on production rate ratio errors for ^{10}Be and ^{26}Al of about ± 7–9%) are not shown. Samples LW 13.3, 14.2 and 24.1 show an unequivocal burial signal, whereas in contrast that for LW 23.2, LW 20.3, LW 18.1 and LW 12.1 are uncertain given that the minimum detectable burial age is 150–200 ka.

LW 14.1 and LW 14.3 on transect B–B') ^{26}Al ages are not available due to laboratory failures in either ICP measurement of aluminium in purified quartz or unacceptably high aluminium concentrations which prevented reliable AMS determination of a $^{26}Al/Al$ ratio.

In general, the oldest ages occur at highest elevations with the youngest ages closest to the present ice surface (Fig. 7), but neither of the two transects show an entirely consistent age-elevation trend. Complexities in the exposure history of erratics, as described above, are clearly evident at Lake Wellman. Despite the observation of increasing age with elevation, these complexities preclude a definitive conclusion to be given regarding the evolution of changes in ice volume of Hatherton glacier. Given the large spread in ages (1–2220 ka), common glacial drifts mapped over different elevation ranges for transects A–A' and B–B', and samples with complex exposure histories, our approach to achieve a plausible and reasonable chronology of Hatherton ice volume changes assumes that selecting either the youngest or oldest ages from each site (or drift) defines the possible end-members of age-elevation models. Basically this means that for a minimum age model, older erratics at lower than expected elevations are presumably due to excessive inheritance, whilst for a maximum age model, younger erratics can appear at higher elevations due to resetting or post-depositional modification. We filter our sample population by first applying a criteria, based on a plot of $^{26}Al/^{10}Be$ ratios versus normalized SLHL ^{10}Be concentrations (Fig. 8), to identify the subset of reworked samples deemed inappropriate for inclusion. Three samples, namely LW 14.2 (sited on the apex of Moraine 2), LW 13.3 and LW 24.1, of the plotted 17 show unequivocal evidence for a complex exposure with burial as the $^{26}Al/^{10}Be$ ratio for these three samples all fall well within the defined burial zone of Fig. 8. For example, LW 14.2 (^{10}Be 415 ± 41 ka; ^{26}Al 254 ± 30 ka) shows a considerable integrated history of pre-exposure, extended burial larger than 0.5 Ma, and an unspecified final stage re-exposure. Within the criteria of overlapping 1σ analytical error for the $^{26}Al/^{10}Be$ ratio and respective 1σ error envelope for the exposure-erosion island (due to ~ 10% uncertainty in production rates), the remaining 14 samples are consistent with an interpretation of continuous exposure. Samples LW 23.1, 24.2, and 25.1 (where ^{10}Be ages are less than 2–3 ka) and LW 02.1 (which has an ^{26}Al age larger than the ^{10}Be age by more than 2σ) are not shown in Fig. 8.

Bentley *et al.* (2006) applied a similar methodology to their exposure ages in a study to measure timing of local LGM and deglaciation of the Antarctic Peninsula. About five of the 29 samples were designated as complex, and of the remaining 24, all but three ranged in age from 7–60 ka. Their smaller age distribution and focus on last deglaciation made their choice of a minimum age model plausible as it is most unlikely to get a post-LGM or late-glacial age younger than last deglaciation. However, for our Lake Wellman dataset, which evidently demonstrates multiple glacial cycles over a far longer period of time and which is restricted to erratics on drift sheets, a maximum age model requires consideration as it appears to be more consistent with the overall field observations and the extended million year exposure age scale than an alternate interpretation based on minimum ages.

We also apply a second filter by rejecting the remaining two of the three samples collected from Transect B–B' at site LW 14 on the surface of an unconsolidated moraine labelled as Moraine 2 in Fig. 2 and pictured in Fig. 4b. The results from LW 14 exhibit the most complexity in exposure age interpretation. We feel this is justified on the basis that a) neither of these two samples is reported with a ^{26}Al age, b) the 3 ^{10}Be ages were collected in very close proximity to each other and range from 16.1 ± 2.0 ka, 192 ± 18 ka to 415 ± 41 ka, and c) Moraine 2 showed strong characteristics of surface modification and deformation being predominately matrix rather than boulder

https://doi.org/10.1017/S0954102010000799 Published online by Cambridge University Press

or clast supported. Most probably Moraine 2 is a composite feature resulting from multiple advances (perhaps over a time period of 30–400 ka) and is undergoing a continuous process of modification. It is interesting to note that the three rejected samples from Moraine 2 can all be considered as small cobbles in comparison to the other metre-sized erratics from transect B–B'.

Exposure age interpretation and chronology of glacial drifts

Isca drift. Based on a maximum age selection, the three samples from LW 11 and LW 09 at the highest elevations, ~ 1575 m, record the oldest ^{10}Be ages of the full dataset; 929 ± 103 ka, 2196 ± 356 and 2275 ± 345 ka, respectively. These two sites lie within undifferentiated drift but their locations, being at the same altitude and directly adjacent to Isca drift, are consistent with a far more extensive volume of Hatherton Glacier during the early–mid Pleistocene suggesting a 1–2 Ma age for Isca. In transect B–B', highest elevation samples at LW 12 (1155 m) give widely different ^{10}Be exposure ages of 128 ± 13 and 395 ± 38 ka (with concordant ^{26}Al ages), the latter exposure age is the oldest of the B–B' transect and is far younger than the oldest A–A' transect age of 2.2 Ma at 1500 m. Although the LW 12 ages are clearly divergent, they demonstrate a minimum glaciation age for Isca drift of between 130–400 ka, equivalent to MIS 6 or MIS 10. With a near ^{26}Al saturation exposure age (at zero erosion) for LW 09.1 and equivalent ^{10}Be age for adjacent sample LW 09.2, it is difficult to explain such old ages to be a result solely of inheritance. Thus we conclude that no ice has advanced over this location for at least the past 1 Ma and more probably over the past 2 Ma.

Danum drift. Two sites at intermediate elevations of ~1100 m are associated with Danum drift; a single sample from LW 15 which lies 1 km off the main axis of transect A–A', and two samples from LW 13 on transect B–B' up-slope and adjacent to Moraine 2. We presume that Moraine 2 marks the ice advance limits of the younger Britannia drift over the older Danum drift. Selection of either a minimum ^{10}Be age of 77 ka for LW 13.2 or a maximum age of 630 ka (LW 15.1) for the Danum drift deposition are both consistent with respect to stratigraphical age increasing with altitude based on the same age model criteria when applied to the Isca drift. However, as LW 15.1 does not lie directly on the main A–A' axis, we tentatively can assign a maximum 230 ka ^{10}Be age from LW 13.3 but note that this sample shows discordant ^{10}Be and ^{26}Al ages.

Britannia drift. Applying the procedure above to estimate a minimum and maximum Britannia drift age from eight available samples (LW 18, 20, 21, transect B–B'; and LW 2, transect A–A') results in a minimum ^{10}Be age of 23 ± 3 ka or maximum of 183 ± 17 ka. Again, these two age boundaries for Britannia drift are consistent with the respective minimum and maximum age boundaries deduced above for the two older Danum and Isca drifts. However, we offer an alternate and sounder estimate for the age of Britannia drift which acknowledges the statistical age distribution or clustering of five of the eight ages. The three pairs of samples from three sites in transect B–B' below the elevation of Moraine 2 were collected along the upper 1 km width of the Britannia drift covering an elevation range of 981–1087 m. Five of these six ^{10}Be ages show a well constrained clustered age range from 29.3 ± 2.7 ka to 43.3 ± 4.1 ka which is statistically consistent with a single population of mean age and 1σ age error of 37.0 ± 5.5 ka and a weighted mean age of 35.6 ± 1.5 ka (± 5%) (a similar result is obtained for the ^{26}Al ages, 35.5 ± 1.9 ka). The single outlier, sample LW 18.3 at 183 ± 17 ka, which actually determines Britannia's 'maximum' age hence appears to be five times larger than the mean Britannia age determined from the other five samples. A second approach to estimating Britannia drift age based on the remaining two samples (LW 2.1 and 2.2 from transect A–A') gives a minimum Britannia age of 23 ± 3 ka (as above) or maximum age of 78 ± 7 ka. These two age limits for Britannia bracket the spread in the ages of the five samples (i.e. 29 to 43 ka) used to calculate the single population mean age.

Hatherton drift. No samples from Hatherton drift were available for collection on transect B–B'. Two of the three lowest elevation sites at ~ 850 m on transect A–A', i.e. LW 23, LW 25, are effectively at the ice contact margin of today's Hatherton Glacier with the shoreline of Lake Wellman. LW 23 samples were taken form the apex of a moraine labelled as Moriane 1 in Fig. 2 and pictured in Fig. 4a. The third site, LW 24 at 895 m, is adjacent to the boundary of Hatherton and Britannia drift and only 50 m above the surface of Lake Wellman. We note that today's elevation of the central axis of Hatherton Glacier is at ~ 960 m. Exposure ages (either ^{10}Be or ^{26}Al) for all six samples (two per site), show a striking complexity in the A–A' transect. The ^{10}Be ages from each pair of samples from each of the three sites are incompatible with each other but interestingly show a bimodal distribution. ^{10}Be ages for three of the samples cluster together between 0.8 and 2.6 ka, whereas two others are 14.8 ± 1.3 and 19.1 ± 1.7 ka. Respective ^{26}Al ages for each of these five samples show a similar pattern. The sixth sample, LW 24.1, with a ^{10}Be age of 65.5 ± 6 ka is inconsistent with this trend and shows a distinct burial signal (Fig. 8). Our options for Hatherton drift are, according to a minimum age model, that it is a late Holocene - modern deposition (i.e. younger than 2–3 ka), older ages being rejected due to inheritance equivalent to ~ 15 kyrs. If in turn, the Hatherton drift age is defined by the 14.8 ± 1.3 and 19.1 ± 1.7 ka exposure ages (^{10}Be) of LW 25.2 and LW 23.2 respectively, the near-zero ages are

https://doi.org/10.1017/S0954102010000799 Published online by Cambridge University Press

rejected on the basis of recent exhumation and post-depositional modification. Hence, based on a model of maximum site ages, the last local glacial maximum of Hatherton Glacier occurred between ~15–19 ka. In addition, we favour the older ages for site LW 23 and LW 25 because there is abundant evidence of reworked boulders in the Hatherton drift where striated and weathered surfaces have been fragmented, chipped and fresh surfaces exposed. Choosing the latter option leads to the question of the location of the (global) LGM advance at Lake Wellman because of the eight samples within the next oldest drift, Britannia, only one resembles an LGM age, i.e. ~23 ka (LW 2.2), and five from transect B-B' show a well constrained pre-LGM age for the Britannia drift of 35.6 ± 1.5 ka.

Age models

For both transects A–A' and B–B', the selection of either maximum or minimum ages describe age-elevation trends which are chrono-stratigraphically consistent for the four glacial drift deposits. Cosmogenic exposure ages generally follow a decreasing age trend with decreasing elevation but do not follow the defined chronologic definitions presented by Bockheim *et al*. (1989). Choosing a scenario wherein large-scale inheritance is not the dominant process distorting ages appears to provide overall a more robust and consistent chronostratigraphic interpretation of glacial ice advance. Rejecting samples displaying burial and using a model of maximum ^{10}Be age at given site elevations gives a LGM age (15–20 ka) for Hatherton drift, a MIS 3 (30–40 ka) age for the Britannia drift, an age range of 230 to 630 ka for the Danum drift and at least 395 ka, and more probably 2 Ma, for the Isca drift. The important features we conclude from this interpretation is that multiple glaciations spanning at least the past 2 Ma up to altitudes of 1500 m (or 600 m above present day ice level) have occurred through the Lake Wellman area and ice volume at the LGM may have been considerably smaller than previously assumed and, perhaps, no larger than we observe today. Choosing the alternate minimum age model forces the age scale from Isca to Hatherton drifts to contract into the Last Glacial Cycle (i.e. ~ the last 130 kyrs), places Danum drift at 77 ka (i.e. MIS 4), Britannia drift at 23 ka which precedes by ~2–3 ka the global LGM maximum Antarctic cold period at 19–20 ka (based on Antarctic ice cores) and requires Hatherton glacial expansion in the late Holocene. With this interpretation, ice volume history prior to the last interglacial (or more likely MIS 6 if we include a reasonable erosion rate for exposure age correction) is not recorded at Lake Wellman, and ice volume at LGM would be ~ 300 m higher in elevation than current ice elevation of Hatherton Glacier.

Fig. 9. Bullet shaped rocks. The direction of ice flow with respect to the rock is from left to right. The clasts are strongly faceted and striated and are indicative of warm based ice.

https://doi.org/10.1017/S0954102010000799 Published online by Cambridge University Press

Although the prevalence of inheritance in Antarctic studies is well noted (Stone *et al*. 2003, Bentley *et al*. 2006), the ease of its identification has largely been confined to datasets focussed on LGM or Holocene ice sheet deglaciation, where even short-term recycling of glacial debris can readily result in old-age outliers. In our case, by selecting minimum ages, unreasonable values of inheritance of up to 2 Ma are required. Apart from Isca, estimates of inheritance ages from ~ 20–60 kyr (Hatherton drift samples) or even as large as 150 kyr (Danum drift) would appear to be acceptable, but this conclusion neglects the well-clustered mean exposure age of 35.6 ± 1.5 ka (error in mean) for the five of six Britannia drift samples distributed along transect B–B'. The 1σ age error for these five clustered samples is only ± 5 ka and considering the complexity in age groupings for all other drifts, is our strongest evidence to support our preference for caution in taking minimum ages. Interestingly, it appears in this region where the dominant form of glacial debris is large and extensive drift sheets of heterogeneous-sized matrix, that erratics on the surface of the drift (such as those from sites LW 18, 20 and 21) may offer a more reliable target for cosmogenic exposure age studies than moraines that overly them.

The Lake Wellman area is draped in a substantial but unknown thickness of 'drift' materials. Bedrock outcrops are sparse. All the evidence in the field area suggests that active wet based ice has flowed over the areas examined in this study. The evidence comes from the following sources:

1. The physical appearance and characteristics of some of the individual clasts suggests that material transport was by wet based flow. These include classic bullet shaped clasts with faceted faces and crag and tail features preserved (Fig. 9). These striated bullet shaped rocks and clasts are common in the Lake Wellman area. They occur from the modern ice surface to elevations of 1550 m. Cumulatively they are diagnostic of wet based ice. The remaining evidence is ancillary.
2. The lithologies preserved in all the drifts and moraines include rock types, most notably granite, that do not crop out in the Lake Wellman area indicating transport over large distances (Figs 5 & 6).
3. The preservation of relatively large, very distinct terminal moraines with, in some cases, near angle of repose slopes also supports the interpretation of relatively fast moving ice. These include both symmetrical and asymmetrical ridges, suggesting at least localized push and dump moraines (Fig. 4). In fact, the thick drift sequences themselves are indicative of debris rich ice and again suggest relatively fast flowing erosive ice.
4. The preferred interpretation using the maximum ^{10}Be exposure ages per site suggests that the population of drift material with inheritance is low and failure of older moraine samples to deliver reliable ages due to active surface modification; both support wet based ice passage. The thick carpet of glacial drift may represent basal debris whereas the linear moraine ridges most likely represent supraglacial material.

We cannot, of course, discount the possibility that some advances, or parts thereof, may be cold based, but the evidence for wet based ice in this area at some stages in its history is convincing.

Implications of the chronology for glacial history and diversity

At its maximum ice extent ~ 2.2 million years ago in the Pliocene, ice was at least ~ 1650 m a.s.l. or 800 m above the present surface of Lake Wellman which, in reference to the modern ice surface of Hatherton Glacier, is equivalent to 690 m increase in ice thickness. We suggest, based on the volume and extent of glacial debris that warm based ice blanketed the whole area at this time. We do not rule out readvances of the ice, and the discordant ages of Isca drift material between the two transects suggests that the lower elevation Isca site on transect B was re-occupied by ice ~ 400 ka in the mid- to late-Pleistocene and that a single designation for this drift may be somewhat unhelpful. The deposition age for Danum drift is not well constrained from our dataset, but according to our preferred interpretation, appears to be ~ 630 ka, although a Late Quaternary age (~ 75 ka) cannot be discounted from our data. Moraine 2, at an elevation of 1115 m a.s.l. (~ only 60 m above present day Hatherton ice surface), if deposited by Britannia drift at ~ 35 ka indicates the extent of increased ice thickness during the last major ice expansion in this area. This is 500 m lower compared to the ice thickness recorded by the major overriding ice event in the mid Pliocene. Our strongest constraint on the Britannia Drift, downhill of this ridge comes from the tightly clumped five ages of LW 18, 20, and 21 of 35 ± 5 ka. This is highly compatible with observations from elsewhere in East Antarctica that demonstrate maximum last glaciation ice extent well before the LGM (Gore *et al*. 2001).

The LGM limit appears to be restricted to the Hatherton drift whose upper limits are at an elevation just 50 m above the modern ice sheet surface. This indicates that LGM ice increase at this location was a minor phenomenon. In fact there is no conclusive evidence that LGM ice was ever above modern limits as the pre-Holocene ages from LW 23 and 25 are deglaciation ages and may relate to a post-LGM thickening as precipitation increased on the polar plateau after the end of the cold dry LGM phase.

The spatial resolution of glacial models and ice volume reconstructions has failed to detect the geographical distribution of glacial refugia (ice-free) in Antarctica. Clearly, the terrestrial biota indicates that refugia were more widespread and provides novel constraints that can be highly informative for reconstructing the past glacial history of Antarctica (Stevens *et al*. 2006, Convey & Stevens 2007, Convey *et al*. 2009). For many areas of the continent there are no field data estimates for previous ice sheet thicknesses (Bentley *et al*. 2006) which restrict our ability to identify potential refugial locations or regions. Notable exceptions include the Dry Valleys of the Transantarctic Mountains of southern Victoria Land, where geomorphology supports ice-free conditions throughout the last 12–10 Ma (Sugden *et al*. 2006).

Much of what we know about the terrestrial biodiversity comes from the Dry Valley region yet other regions, such as in northern Victoria Land and the Beardmore and Shackleton glaciers, show similarly isolated biological signals (Brundin 1970, Adams *et al*. 2006, Stevens & Hogg 2006, Stevens *et al*. 2007). Indications from the Darwin Mountains, however, show that overall biota was sparse (see also Ruprecht *et al*. 2010). The significance of limited biodiversity (diversity and abundance) may not immediately seem obvious. However, a lack of biotic presence integrated with the Darwin Mountains glacial history shown here does in fact tell us a lot about the requirements necessary for colonization (and persistence) of flora and fauna associated with Antarctic soils, and these links provide a critical step forward in understanding the requirements and persistence of terrestrial life in Antarctica.

The paradigm of eradication of terrestrial biota during glacial maxima has been questioned (Stevens *et al*. 2006, Convey *et al*. 2009) and suggestions made for interdisciplinary research to integrate across geology, glaciology and biology (Convey *et al*. 2008, 2009). The Lake Wellman area shows a great deal of habitat modification with ice thickness ~ 800 m higher than its current level with some of the terrain ice-free for up to two million years, indicating that the glacial eradication dominated and did not support significant refugia for Antarctic terrestrial biota. This conclusion also has implications for the length of time required for terrestrial biota to recolonize post-glacial retreat and the gradual sequence (succession) of recolonizers necessary to 'prepare' a viable habitat in Antarctica; a question that has not been addressed in Antarctica.

Conclusions

We have successfully applied the technique of cosmogenic surface exposure dating in the Lake Wellman region of the Hatherton Glacier, East Antarctica, resulting in a constrained glacial chronology that spans the last two million years of glaciations. Geomorphic field observations show that active ice (perhaps wet based) has scoured the region transporting boulders and depositing thick drift sheets over numerous glacial cycles. From the set of 25 erratics from two orthogonal altitudinal transects, 16 provided paired ^{10}Be and ^{26}Al ages that confirm a simple continuous period of exposure (four failed to give a ^{26}Al age). Their mean exposure ages increase as a function of increasing elevation above current ice sheet surface, indicating a long-term decrease in ice volume of the Antarctic ice sheet moving over the Transantarctic Mountains since the Late Pliocene.

In contrast to mid-latitude, temperate alpine glacial systems, the frequency of erratics in the Polar Regions with a considerable degree of inheritance or burial histories resulting from preservation of multiple exposure periods and reworking of pre-exposed sub-glacial debris, respectively, can be significant. This will always limit the reliability of interpretations. Nevertheless, based on two simple age models - choosing the youngest erratic age at each elevation site or the oldest, there are sufficient reliable results to substantially modify the indirect chronology of Bockheim *et al*. (1989). We conclude that:

- The maximum recorded ice thickness of the Hatherton Glacier in the Lake Wellman area was at least 690 m thicker than today's elevation of the Hatherton Glacier surface. The oldest drift (Isca) was deposited by a Pliocene advance of an outlet glacier of the East Antarctic Ice Sheet more than 2.2 million years ago. The next youngest drift, Danum drift, based on a maximum age scenario, was deposited at ~ 630 ka, but an age commensurate with MIS 4 at approximately 75 ka is also possible.
- In contrast to these older drifts, the Britannia drift is relatively well constrained by our data. It clearly indicates that the last substantial thickening of ice in this area occurred at ~ 35 ka, or more precisely between ~ 45 ka to ~ 30 ka during MIS 3, with the ice thinning progressively after that time. According to the elevation spread of the ages from the Britannia drift, the ice thickness at MIS 3 was not that much different from that during the Danum glaciation.
- Independent of the assumptions of age model distributions, ice volume changes from LGM through to the late Holocene are represented at Wellman by the youngest and smallest surface area drift - the Hatherton drift. Accordingly, using maximum ages per site, the increase in ice volume at the global LGM or during the last inter-glacial transition from 20–10 ka, can at most result in an ice thickness 50 m larger than the modern ice sheet surface. The set of minimum exposure ages on the Hatherton drift range from ~ 0.5 to ~ 3 ka and hence we cannot rule out the possibility that the Hatherton drift is a late Holocene deglaciation event. All these data suggest that ice at the LGM in the Lake Wellman area was substantially less thick than previously postulated.

Acknowledgements

We are very grateful to the excellent field support from Antarctica New Zealand as part of the Latitudinal Gradient

Project (LGP). In particular, we thank S. Gordon, I. Millar, R. Türk and M. Knox for logistics and/or field planning and assistance. We also thank Paul Brody for identification of algae. We are very grateful to the reviewers who provided very useful suggestions to improve the manuscript. We acknowledge financial support for this work from AINSE and from ANSTO's CcASH project 0203v (Cosmogenic Climate Archives of the Southern Hemisphere).

References

Adams, B.J., Bardgett, R.D., Ayres, E., Wall, D.H., Aislabe, J., Bamforth, S., Bargagli, R., Cary, C., Cavacini, P., Connell, L., Convey, P., Fell, J.W., Frati, F., Hogg, I.D., Newsham, K.K., O'donnel, A., Russell, N., Seppelt, R.D. & Stevens, M.I. 2006. Diversity and distribution of Victoria Land biota. *Soil Biology and Biochemistry*, **38**, 3003–3018.

Balco, G., Stone, J.O., Lifton, N.A. & Dunai, T.J. 2008. A complete and easily accessible means of calculating surface exposure ages or erosion rates from ^{10}Be and ^{26}Al measurements. *Quaternary Geochronology*, **3**, 174–195.

Bentley, M.J. 1999. Volume of Antarctic ice at the Last Glacial Maximum and its impact on global sea level change. *Quaternary Science Reviews*, **18**, 1569–1595.

Bentley, M.J., Fogwill, C.J., Kubik, P.W. & Sugden, D.E. 2006. Geomorphological evidence and cosmogenic 10Be/26Al exposure ages for the Last Glacial Maximum and deglaciation of the Antarctic Peninsula Ice Sheet. *Geological Society of America Bulletin*, **118**, 1149–1159.

Bockheim, J.G., Wilson, S.C., Denton, G.H., Andersen, B.G. & Stuiver, M. 1989. Late Quaternary ice-surface fluctuations of Hatherton Glacier, Transantarctic Mountains. *Quaternary Research*, **31**, 229–254.

Briner, J.P., Kaufman, D.S., Manley, W.F., Finkel, R.C. & Caffee, M.W. 2005. Cosmogenic exposure dating of late Pleistocene moraine stabilization in Alaska. *Geological Society of America Bulletin*, **117**, 1108–1120.

Briner, J.P., Miller, G.H., Davis, P.T., Bierman, P.R. & Caffee, M. 2003. Last Glacial Maximum ice sheet dynamics in Arctic Canada inferred from young erratics perched on ancient tors. *Quaternary Science Reviews*, **22**, 437–444.

Brundin, L. 1970. Antarctic land faunas and their history. *In* Holdgate, M.W., *ed. Antarctic ecology*. London: Academic Press, 41–54.

Butler, E.R.T. 1999. Process environments on modern and raised beaches in McMurdo Sound, Antarctica. *Marine Geology*, **162**, 105–120.

Child, D., Elliot, G., Mifsud, C., Smith, A.M. & Fink, D. 2000. Sample processing for earth science studies at ANTARES. *Nuclear Instruments & Methods in Physics Research*, **172**, 856–860.

Convey, P. & Stevens, M.I. 2007. Antarctic biodiversity. *Science*, **317**, 1877–1878.

Convey, P., Gibson, J.A.E., Hillenbrand, C.-D., Hodgson, D.A., Pugh, P.J.A., Smellie, J.L. & Stevens, M.I. 2008. Antarctic terrestrial life; challenging the history of the frozen continent? *Biological Reviews*, **83**, 103–117.

Convey, P., Stevens, M.I., Hodgson, D.A., Smellie, J.L., Hillenbrand, C.-D., Barnes, D.K.A., Clarke, A., Pugh, P.J.A., Linse, K. & Cary, C. 2009. Exploring biological constraints on the glacial history of Antarctica. *Quaternary Science Reviews*, **28**, 3035–3048.

Conway, H., Hall, B.L., Denton, G.H., Gades, A.M. & Waddington, E.D. 1999. Past and future grounding-line retreat of the West Antarctic Ice Sheet. *Science*, **286**, 280–283.

Denton, G.H. & Hughes, T.J. 2002. Reconstructing the Antarctic Ice Sheet at the Last Glacial Maximum. *Quaternary Science Reviews*, **21**, 193–202.

Fabel, D., Fink, D., Fredinc, O., Harbord, J., Land, M. & Stroeven, A.P. 2006. Exposure ages from relict lateral moraines overridden by the Fennoscandian ice sheet. *Quaternary Research*, **65**, 136–146.

Fink, D. & Smith, A. 2007. An inter-comparison of ^{10}Be and ^{26}Al AMS reference standards and the ^{10}Be half-life. *Nuclear Instruments and Methods in Physics Research*, **B259**, 600–609.

Fink, D., McKelvey, B., Hambrey, M., Fabel, D. & Brown, R. 2006. Pleistocene deglaciation chronology of the Radok Lake basin, Amery Oasis, northern Prince Charles Mountains, Antarctica. *Planetary Science Letters*, **243**, 229–243.

Gosse, J.C. & Phillips, F.M. 2001. Terrestrial *in situ* cosmogenic nuclides: theory and application. *Quaternary Science Reviews*, **20**, 1475–1560.

Gore, D.B., Rhodes, E.J., Augustinus, P.C., Leishman, M.R., Colhoun, E.A. & Rees-Jones, J. 2001. Bunger Hills, East Antarctica: ice free at the Last Glacial Maximum. *Geology*, **29**, 1103–1106.

Haskell, T.R., Kennett, J.P. & Prebble, W.M. 1964. Basement and sedimentary geology of the Darwin Glacier area. *In* Adie, R.J., *ed. Antarctic geology*. Amsterdam: North-Holland Publishing Company, 348–351.

Hood, D. 2010. *The Pleistocene glacial history of the Lake Wellman area, Darwin Mountains, Antarctica*. MSc thesis, Department of Geological Sciences, University of Canterbury, Christchurch, New Zealand, 168 pp. [Unpublished].

Howard-Williams, C., Peterson, D., Lyons, W.B., Cattaneo-Vietti, R. & Gordon, S. 2006. Measuring ecosystem response in a rapidly changing environment: the Latitudinal Gradient Project. *Antarctic Science*, **18**, 465–471.

Huybrechts, P. 2002. Sea-level changes at the LGM from ice-dynamic reconstructions of the Greenland and Antarctic ice sheets during the glacial cycles. *Quaternary Science Reviews*, **21**, 203–231.

Korschinek, G., Bergmaier, A., Faestermann, T., Gerstmann, U.C., Knie, K., Rugel, G., Wallner, A., Dillmann, I., Dollinger, G., von Gostomski, C.L., Kossert, K., Maiti, M., Poutivtsev, M. & Remmert, A. 2009. A new value for the half-life of ^{10}Be by heavy-ion elastic recoil detection and liquid scintillation counting. *Nuclear Instruments and Methods in Physics Research, B*, **268**, 187–191.

Lilly, K., Fink, D., Fabel, D. & Lambek, K. 2010. Pleistocene dynamics of the interior East Antarctic ice sheet. *Geology*, **38**, 703–706.

Mackintosh, A., White, D., Fink, D., Gore, D.B., Pickard, J. & Fanning, P.C. 2007. Exposure ages from mountain dipsticks in Mac. Robertson Land, East Antarctica, indicate little change in ice-sheet thickness since the Last Glacial Maximum. *Geology*, **35**, 551–554.

Miller, G.H., Wolfe, A.P., Steig, E.J., Sauer, P.E., Kaplan, M.R. & Briner, J.P. 2002. The Goldilocks dilemma: big ice, little ice, or "just-right" ice in the eastern Canadian Arctic. *Quaternary Science Reviews*, **21**, 33–48.

Nakada, M. & Lambeck, K. 1988. The melting history of the late Pleistocene Antarctic ice sheet. *Nature*, **333**, 36–40.

Nishiizumi, K., Imamura, M., Caffee, M.W., Southon, J.R., Finkel, R.C. & McAninch, J. 2007. Absolute calibration of ^{10}Be AMS standards. *Nuclear Instruments and Methods in Physics Research*, **B258**, 403–413.

Putkonen, J. & Swanson, T. 2003. Accuracy of cosmogenic ages for moraines. *Quaternary Research*, **59**, 255–261.

Ruprecht, U., Lumbsch, H.T., Brunauer, G., Green, T.G.A. & Türk, R. 2010. Diversity of *Lecidea* (Lecideaceae, Ascomycota) species revealed by molecular data and morphological characters. *Antarctic Science*, **21**, 10.1017/S0954102010000477.

Stevens, M. & Hogg, I.D. 2006. Contrasting levels of mitochondrial DNA variability between mites (Penthalodidae) and sprigtails (Hypogastruridae) from the Trans-Antarctic Mountains suggest long-term effects of glaciation and life history on substitution rates, and speciation processes. *Soil Biology & Biochemistry*, **38**, 3171–3180.

Stevens, M.I., Greenslade, P., Hogg, I.D. & Sunnucks, P. 2006. Southern Hemisphere springtails: could any have survived glaciation of Antarctica? *Molecular Biology & Evolution*, **23**, 874–882.

Stevens, M.I., Frati, F., McGaughran, A., Spinsanti, G. & Hogg, I.D. 2007. Phylogeographic structure suggests multiple glacial refugia in northern Victoria Land for the endemic Antarctic springtail *Desoria klovstadi*, (Collembola, Isotomidae). *Zoologica Scripta*, **36**, 201–212.

Stone, J.O. 2000. Air pressure and cosmogenic isotope production. *Journal of Geophysical Research*, **105**, 753–759.

Stone, J.O., Balco, G.A., Sugden, D.E., Caffee, M.W., Sass, L.C., Cowdery, S.G. & Siddoway, C. 2003. Holocene deglaciation of Marie Byrd Land, West Antarctica. *Science*, **299**, 99–102.

Stroeven, A.P., Fabel, D., Hättestrand, C. & Harbor, J. 2002. A relict landscape in the centre of Fennoscandian glaciation: cosmogenic radionuclide evidence of tors preserved through multiple glacial cycles. *Geomorphology*, **44**, 145–154.

Sugden, D.E., Bentley, M.J. & Cofaigh, C.Ó. 2006. Geological and geomorphological insights into Antarctic ice sheet evolution. *Philosophical Transactions of the Royal Society*, **A364**, 1607–1625.

Sugden, D.E., Balco, G., Cowdery, S.G., Stone, J.O. & Sass, L.C. 2005. Selective glacial erosion and weathering zones in the coastal mountains of Marie Byrd Land, Antarctica. *Geomorphology*, **67**, 317–334.